

Mechanical Properties of Doubly Stabilized Microtubule Filaments

Taviare L. Hawkins,^{†‡} David Sept,[§] Binyam Mogessie,[¶] Anne Straube,[¶] and Jennifer L. Ross^{†*}

[†]Department of Physics, University of Massachusetts Amherst, Amherst, Massachusetts; [‡]Department of Physics, University of Wisconsin-La Crosse, La Crosse, Wisconsin; [§]Department of Biomedical Engineering, University of Michigan, Ann Arbor, Michigan; and [¶]Centre for Mechanochemical Cell Biology, Warwick Medical School, University of Warwick, Coventry, United Kingdom

ABSTRACT Microtubules are cytoskeletal filaments responsible for cell morphology and intracellular organization. Their dynamical and mechanical properties are regulated through the nucleotide state of the tubulin dimers and the binding of drugs and/or microtubule-associated proteins. Interestingly, microtubule-stabilizing factors have differential effects on microtubule mechanics, but whether stabilizers have cumulative effects on mechanics or whether one effect dominates another is not clear. This is especially important for the chemotherapeutic drug Taxol, an important anticancer agent and the only known stabilizer that reduces the rigidity of microtubules. First, we ask whether Taxol will combine additively with another stabilizer or whether one stabilizer will dominate another. We call microtubules in the presence of Taxol and another stabilizer, doubly stabilized. Second, since Taxol is often added to a number of cell types for therapeutic purposes, it is important from a biomedical perspective to understand how Taxol added to these systems affects the mechanical properties in treated cells. To address these questions, we use the method of freely fluctuating filaments with our recently developed analysis technique of bootstrapping to determine the distribution of persistence lengths of a large population of microtubules treated with different stabilizers, including Taxol, guanosine-5' [(α , β)-methylene] triphosphate, guanosine-5'-O-(3-thiotriphosphate), tau, and MAP4. We find that combinations of these stabilizers have novel effects on the mechanical properties of microtubules.

INTRODUCTION

The microtubule cytoskeleton is a chemomechanical network based on microtubule filaments supplemented with a number of regulatory accessory proteins, called microtubule-associated proteins (MAPs). This network is vital for important cellular processes such as morphology and differentiation, intracellular organization, and mitosis. The mechanical stiffness of individual microtubules controls the mechanical properties of the network, and it is modified for different functions in the cell. For instance, it would be favorable for the stable microtubules of the axon to be stiff and straight to support the extended structure required for long-distance axonal transport. Conversely, microtubules in a proliferating cell should be dynamic and flexible to enable rapid redistribution during transitions between interphase and mitosis.

There are a number of microtubule-stabilizing agents that control microtubule dynamics and affect their mechanical properties, including drugs, nucleotides, and associated proteins. Interestingly, Taxol, a microtubule-stabilizing drug used in chemotherapy, is the only known stabilizer to make microtubules more flexible (1–7). Conversely, guanosine-5' [(α , β)-methylene] triphosphate sodium salt (GMPCPP) is a slowly hydrolyzable GTP analog that stabilizes and stiffens microtubules (6,8,9). We are interested in the effects of doubly stabilized microtubules that are polymerized with GMPCPP and then stabilized with Taxol

since these microtubules have been shown to be resistant to depolymerization by kinesin-8 motors (10). We want to determine whether the mechanical perturbations induced by Taxol and GMPCPP are additive or cooperative, or whether the effect of one dominates that of the other. We also test the effects of guanosine-5'-O-(3-thiotriphosphate) (GTP- γ -S), a nonhydrolyzable GTP analog recently reported to mimic the tip structure of microtubules for the end-binding (EB) proteins (11).

MAPs are known to regulate the nucleation, polymerization, stability, and mechanical properties of microtubules in cells. In particular, much attention has been paid to the stabilizing MAPs of neuronal cells, especially tau proteins, because of their importance in cell structure and neuronal disease (12,13). Tau is an important neuronal MAP known to nucleate, enhance the growth of, and stabilize microtubules both in cells and in vitro (12,14–21). Tau is found in the axons of neurons and needs to mechanically stabilize and stiffen microtubules to enable axonal microtubules to support the long, extended structure of the axon. It has been demonstrated that tau stiffens microtubules in vivo and in vitro when added to already polymerized microtubules (4,9). However, in the cell, tau is likely to be present during polymerization. We want to determine whether polymerizing in the presence of tau alters the mechanical properties in a different way. The question of tau presence during polymerization is even more interesting in light of recent reports that it has two microtubule-binding sites: one on the microtubule exterior and the other on the microtubule lumen near the Taxol-binding site (22). Tau and Taxol appear to compete for the interior site, but tau cannot reach

Submitted July 15, 2012, and accepted for publication February 19, 2013.

*Correspondence: rossj@physics.umass.edu

Binyam Mogessie's present address is MRC Laboratory of Molecular Biology, Cambridge, United Kingdom.

Editor: David Odde.

© 2013 by the Biophysical Society
0006-3495/13/04/1517/12 \$2.00



the interior site when added postpolymerization. To investigate the effects of tau binding to the interior site, we measure the rigidity of microtubules copolymerized with tau present and compare the results to microtubules with tau added after polymerization and Taxol stabilization.

Compared to tau, less is known about MAP4, the MAP found in the neuronal cell body and, in contrast to tau, ubiquitously expressed in a variety of nonneuronal tissues. Due to the similar microtubule-binding sequence, many have speculated that MAP4 will have the same effects on microtubule nucleation, stabilization, and mechanics as tau and MAP2. Indeed, MAP4 appears to protect microtubules and enhance growth of microtubules in vivo (23,24) and has been shown to stabilize microtubules by inducing rescue events in vitro (25,26). Cells express three major MAP4 isoforms that share the same microtubule-binding domain, but have very different projection domains (27,28). The muscle-specific isoform mMAP4 contains a 120-kDa insertion in the projection domain of the ubiquitously expressed uMAP4 (28). Species-wide sequence data reveal a third variant, oMAP4, expressed in brain, eye, heart, and skeletal muscle, and includes a unique 50-kDa projection domain (29,30). In addition, MAP4 isoforms vary in the number of tau-like microtubule binding repeats. MAP4 variants with three, four, and five repeats are expressed in cells (31) and confer different properties. For example, five repeats are required for MAP4 to act as roadblocks for kinesin (32), whereas a three-repeat uMAP4 is sufficient to limit force generation by dynein (33). Here, we measure, for the first time to our knowledge, the effects of a tau-like four-repeat isoform of oMAP4 on microtubule mechanics in the presence of Taxol.

In this study, we explore the competitive effects of multiple types of stabilization on the mechanical properties of microtubules. We use the thermal fluctuation method with Fourier decomposition, as described previously (34,35). Further, we use the bootstrapping method we recently developed to estimate error in our measurement, and we perform a weighted fit to the normal modes to determine the persistence length of individual microtubules (34). We take a large data set for each experimental parameter to enable comparisons between the distributions of persistence length, instead of comparing the average value of persistence length, which can be misleading due to the log-normal nature of the distributions (34). We find that GMPCPP microtubules have enhanced stiffness, and that the effect dominates that of Taxol, whereas GTP- γ -S reduces microtubule rigidity to an extent similar to that seen with Taxol. We also find that there is an effect of adding the tau protein during polymerization, but that adding it after Taxol stabilization, even at very high concentrations, has little effect on the mechanical properties of microtubules. Finally, we find that MAP4 does not change the average persistence length of microtubules but does significantly alter the shape of the distribution of persistence lengths, causing a reduction in the asymmetry

and width of the log-normal distribution and making it appear Gaussian. These data report on the different mechanisms of stabilization and offer insight into how mechanics can relate to the structural changes imparted by stabilizers.

MATERIALS AND METHODS

Reagents and microtubules

All chemical reagents were purchased from Sigma (St. Louis, MO) unless otherwise stated. Unlabeled porcine tubulin was purified as previously described (34) using the method of Pelouquin et al. (36). Rhodamine-labeled porcine tubulin was purchased as lyophilized powder (TL590M, lot 015, Cytoskeleton, Denver, CO). Rhodamine tubulin was resuspended at 5 mg/ml in PEM-100 (100 mM PIPES, pH 6.8 with KOH, 2 mM EGTA, and 1 mM MgSO₄) and added to unlabeled tubulin at a ratio of 1:5 (rhodamine/total). Tubulin was centrifuged at 298,000 $\times g$ at 4°C to remove any aggregated tubulin. Microtubules were polymerized in the presence of 1 mM GTP for 20 min at 37°C. For microtubules stabilized by paclitaxel (Taxol), 50 μ M was added after polymerization and microtubules were incubated for an additional 20 min at 37°C to equilibrate the Taxol. Microtubules were centrifuged at 14,000 $\times g$ for 10 min at 25°C to remove any unpolymerized tubulin, and the pellet was resuspended in PEM-100 (with 50 μ M Taxol if Taxol was used). Microtubules were incubated at 37°C for 1 h or until they were within the 5–30 μ m length range. GMPCPP microtubules were made as outlined above, except 1 mM guanosine-5' [(α , β)-methylene] triphosphate sodium salt (GMPCPP) was added instead of GTP. GMPCPP microtubules were stable with and without Taxol. Guanosine-5'-O-(3-thiotriphosphate) tetralithium salt (GTP- γ -S) microtubules were made as above, except that 1 mM GTP- γ -S was added instead of GTP. Taxol was required to polymerize GTP- γ -S microtubules. To test GTP- γ -S microtubules without Taxol, we made microtubules with GTP- γ -S in the presence of only 5 μ M Taxol, as described above. The microtubules were then diluted in PEM-100 buffer without Taxol at a 6 times volume. Next the microtubules were pelleted to separate them from the Taxol in solution and resuspended in PEM-100 without Taxol. We performed the dilution and pelleting twice. After the final round of pelleting, we resuspended the pellet in the original volume of PEM-100 without Taxol.

Microtubule-associated proteins

MAPs were expressed and purified from bacteria. The full-length tau protein, denoted 4RL, was purified as previously described (37,38). Briefly, tau was induced with 0.5 mM isopropyl- β -D-thiogalactoside in *Escherichia coli* strain BL21-CodonPlus-(DE3). We lysed bacteria by sonication, and we boiled the supernatant of the lysate to aggregate free proteins. Tau remained in solution after boiling and was separated by centrifugation. Purity was established by sodium dodecyl sulfate polyacrylamide gel electrophoresis with Coomassie blue staining.

The four-repeat version of oMAP4 (accession no. AK146790) was amplified from cDNA of 48 h differentiated C2C12 myoblasts, and cloned to pRSET-A and to pEGFP-C1. GFP-oMAP4 was then also transferred to pRSET-A. 6 \times His-oMAP4 and 6 \times His-eGFP-oMAP4 were expressed in *E. coli* BL21-CodonPlus-(DE3) and purified as previously described for uMAP4 (33). Briefly, bacteria were lysed by sonication, and the free proteins bound to Ni-NTA resin (Qiagen, Germantown, MD) and eluted with 250 mM imidazole. The MAP4-containing fractions were loaded on SP fast-flow sepharose (GE Healthcare, Waukesha, WI), washed with low-salt buffer, and eluted with a step gradient of high-salt buffer (20 mM MES, pH 6.8, 1 mM EGTA, 0.5 mM MgCl₂, and 1 M NaCl) and buffer exchanged to BRB-80 (80 mM PIPES, pH 6.8, 1 mM MgCl₂, 1 mM EGTA).

Tau-stabilized microtubules

Tau-bound microtubules were created in one of two ways. First, microtubules were made as described above, stabilized with Taxol, and then 450 nM tau was added to a 100-fold dilution of 45 μM stock microtubules (final concentration 450 nM tubulin) before for imaging. Thus, the tubulin was at a ratio of 1 to 1, tau to tubulin. We call these microtubules postpolymerization. Second, microtubules were polymerized at 45 μM in the presence of 450 nM tau added with GTP (final ratio 1:100, tau:tubulin). As for other microtubules, Taxol was added after polymerization at 50 μM and a second incubation step was used to equilibrate the Taxol. As above, 450 nM tau was added to a 100-fold dilution of 45 μM stock microtubules (final concentration 450 nM tubulin) before imaging. Thus, the final tubulin to tau ratio was 1 to 1 to ensure microtubule stability. We call these microtubules copolymerization. Microtubules were incubated at 37°C for 20 min up to 2 hr prior to use in assays.

Microtubules with MAP4

We attempted to create MAP4-bound microtubules using the same two methods as described for tau. Unfortunately, MAP4 added during polymerization inhibited nucleation and few microtubules were formed, even when Taxol was added. Thus, MAP4 microtubules were only of the MAP4 postpolymerization variety. Final concentration of 230 nM MAP4 was incubated with 450 nM microtubules, giving a MAP/tubulin ratio of 1:2 during the experiment.

Microtubule flexibility measurements and data analysis

To measure the microtubule flexibility, we performed the same methods described in our recent publication (34). Briefly, microtubules were placed in a very thin (<3 μm thick) chamber made from a slide and coverslip coated with κ -casein to prevent microtubules from adhering to the glass surfaces. Microtubules were imaged in epifluorescence using a Ti-E microscope with 60 \times , 1.49 NA objective (Nikon) and an electron-multiplying CCD camera (Andor) as they fluctuated in two dimensions, and time-lapse movies were recorded using the Nikon Elements software (Nikon). Individual microtubule images were cropped and rotated to horizontal. MatLab was employed to skeletonize and divide the microtubule into 25 segments. The filament shape was decomposed into Fourier modes, as previously described (34,35). The average variance and the error in that variance for the first 25 Fourier modes were determined as previously described using our resampling bootstrap analysis (34). We performed a weighted fit to all the data using the equation

$$\text{var}(a_n) = \left(\frac{L_C}{n\pi}\right)^2 \frac{1}{L_p} + \frac{4}{L_C} \langle \epsilon_k^2 \rangle \left[1 + (N-1) \sin^2 \frac{n\pi}{2N}\right], \quad (1)$$

where $\text{var}(a_n)$ is the variance of the amplitude, a , of the n th normal mode, L_C is the contour length, and N is the number of segments taken along the microtubule. L_p is the persistence length, $\langle \epsilon_k^2 \rangle$ is the noise floor, and both are the fit parameters of the equation.

Statistical analysis

We collected data on 30–50 microtubules for each individual experiment, although not all were analyzable due to noise or other issues. The number of microtubules used for each is quoted in Table 1. We demonstrated previously that the distribution of persistence lengths is log-normal for Taxol-stabilized microtubules (34). We consider this microtubule data our control data, to which we will compare the effects of nucleotides and MAPs. To compare experimental data sets to control, we used several techniques.

First, we log-transformed the data before binning to make the histograms. The effect of log-transforming the data is to create normal, Gaussian distributions from log-normal data, and these can be directly compared using the standard Student's t -test (34). We fit the data sets to Gaussian functions of the form

$$A \exp\left(-\frac{(x-x_0)^2}{2\sigma^2}\right), \quad (2)$$

where A is the amplitude, x_0 is the mean of the distribution, and σ is the standard deviation of the distribution.

The second method was to create normalized cumulative distributions of the data. The benefit of cumulative distributions is that there is no binning, and all the data are represented. To compare data sets of cumulative distributions, we used an online application that performs a Kolmogorov-Smirnov test (K-S test) (40) and the statistical package, R (41). A K-S test determines whether two data sets differ significantly without making assumptions about the type of distribution. The K-S test determines the D-statistic for two distributions. The D-statistic is the maximum distance in the probability between two cumulative distributions. In our data table, we report the D-statistic and the resulting probability (p -value) that the two distributions are the same (Table 1). Thus, as usual, a high p -value means that two distributions are likely the same, and a low p -value implies that two distributions are distinct. In addition to determining the D-statistic and the p -value, the online program and R also predicted the probability that a data set would display a certain type of distribution, such as Gaussian or log-normal.

RESULTS AND DISCUSSION

GMPCPP stiffens microtubules, and its effect dominates over the effect of Taxol

We measured the rigidity of GMPCPP microtubules and microtubules doubly stabilized with GMPCPP and Taxol. For both GMPCPP and doubly stabilized microtubules, we found a large variance in the persistence-length measurements. Similar to our control data set of Taxol-stabilized microtubules, these distributions are both log-normal and conform to a Gaussian after a log transformation (Fig. 1 A). The GMPCPP microtubules had an average persistence length of 1.8 ± 0.5 μm , over three times more rigid than Taxol-stabilized microtubules, which had an average persistence length of 0.6 ± 0.1 μm . The doubly stabilized microtubules, GMPCPP with Taxol, had an average persistence length of 1.9 ± 0.7 μm . The results are summarized in Table 1. Using Student's t -tests to compare the log-transformed data, we find that the probability that the Taxol-stabilized microtubules and the GMPCPP microtubules are the same is 0.09%, and the probability that the Taxol-stabilized microtubules and the GMPCPP with Taxol microtubules are the same is 2%. In the case of GMPCPP microtubules and GMPCPP with Taxol microtubules, the p -value was 0.95; thus, there is no evidence that these distributions differ.

We also created cumulative distributions and performed K-S statistical tests to compare the distributions of persistence lengths of Taxol-stabilized, GMPCPP, and doubly stabilized GMPCPP with Taxol microtubules. From these

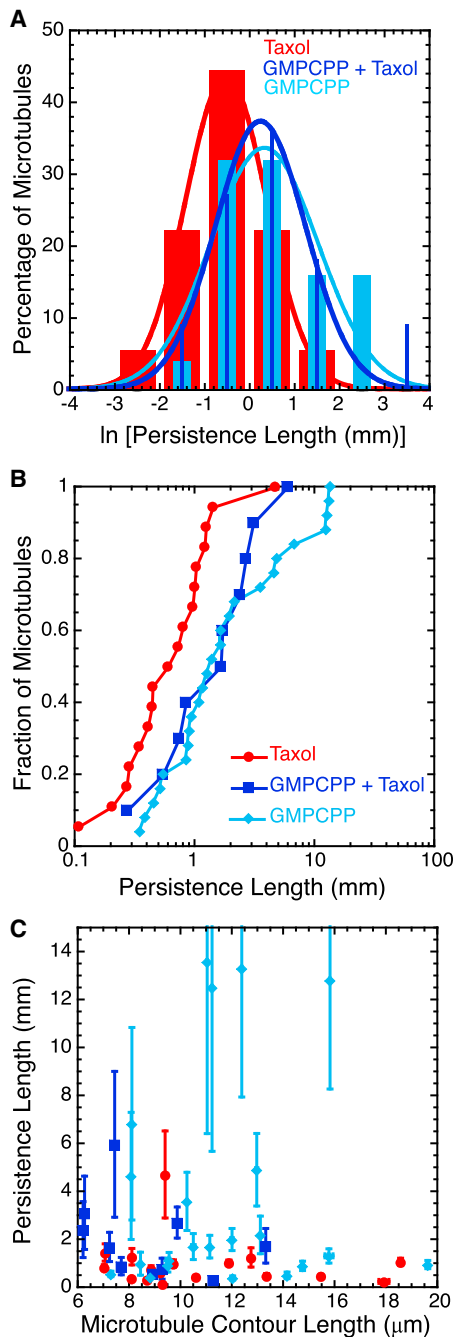


FIGURE 1 GMPCPP dominates over Taxol in its effects on the mechanics of microtubules. (A) Histograms of data after log-transforming the persistence length clearly show differences between Taxol-stabilized microtubules (red bars), GMPCPP-stabilized microtubules (light blue bars), and microtubules doubly stabilized with GMPCPP and Taxol (dark blue bars). In particular, GMPCPP shifts the distribution to longer persistence lengths. We fit the data to Gaussian functions (Eq. 2); fit parameters are given in Table S1. (B) Normalized cumulative distributions of persistence length for Taxol-stabilized microtubules (red circles), GMPCPP-stabilized microtubules (light blue diamonds), and doubly stabilized microtubules (dark blue squares) display significant overlap between the sets of microtubules with GMPCPP, and distinct differences from the Taxol-only data. (C) We see no length dependence of the persistence lengths for Taxol-stabilized microtubules (red circles),

tests, we determine the probability that the Taxol-stabilized and GMPCPP data distributions have a 2% chance of being the same ($D = 0.45$ and $p = 0.02$). The probability that the Taxol-stabilized and doubly stabilized microtubules have the same distribution is only 1% ($D = 0.58$ and $p = 0.01$). Once again, the persistence-length distributions for GMPCPP and GMPCPP with Taxol cannot be differentiated ($D = 0.16$ and $p = 0.98$). We find no statistical evidence that the GMPCPP and the doubly stabilized microtubules are different, implying that the GMPCPP stiffening effect dominates the mechanical nature of microtubules. Further, we note that the persistence length does not depend on the contour length of the microtubules for Taxol, GMPCPP, or doubly stabilized microtubules (Fig. 1 C).

Previous work has measured the persistence length of GMPCPP microtubules by two different thermal fluctuation methods. First, Mickey et al. used the same freely fluctuating filament method that we use here, but without the bootstrapping error analysis and the weighted fitting we perform (9). They found that GMPCPP-stabilized microtubules had a twofold higher persistence length compared to Taxol-stabilized microtubules (14.5 mm for GMPCPP and 7.5 mm for Taxol) (9). Yet these persistence-length measurements are much higher than those measured for Taxol-stabilized microtubules by other groups. Further, to our knowledge, this is the only report to say that Taxol stiffens microtubules compared to unstabilized microtubules (9). There are six other experimental reports that measured both unstable microtubules and Taxol-stabilized microtubules, all of which find that Taxol makes microtubules more flexible (1–6). In addition, theoretical estimates based on molecular dynamics simulations using detailed structural data are consistent with Taxol increasing the flexibility of microtubules (7).

A second study used a thermal-fluctuation method with one end adhered to a surface to measure the persistence length of microtubules without stabilization, with GMPCPP, and with Taxol, each separately (6). The authors found that the GMPCPP microtubules were the stiffest at all temperatures at which stiffness was measured and that the Taxol-stabilized microtubules were always the most flexible; the unstabilized microtubule stiffness was in between. Further, they demonstrated a linear-length-dependent persistence length for the unstabilized and the GMPCPP microtubules, but not for the Taxol-stabilized microtubules. The increased persistence length observed by Kawaguchi et al. is more modest than the length dependence demonstrated by Pampaloni et al. (6,42). In our data, we never observe a length-dependent persistence length, and this could be an effect of the assay used (Fig. S1). Both of the

GMPCPP-stabilized microtubules (light blue squares), or doubly stabilized microtubules (dark blue squares). Error bars represent the mean \pm SE. The numbers of microtubules in each distribution are given in Table 1.

TABLE 1 Mean persistence lengths for stabilized microtubules imaged at 25°C

Nucleotide	Stabilization method	Average flexural rigidity, EI ($\times 10^{-24}$ nm ²)	Average persistence length (mm)	N	D-statistic and p -value (compared to Taxol)
GTP	50 μ M Taxol	2.5 \pm 0.5	0.6 \pm 0.1	18	N/A
GMPCPP	GMPCPP	8 \pm 2	1.8 \pm 0.5	25	$D = 0.45$ $p = 0.02$
GMPCPP	GMPCPP; 50 μ M Taxol	8 \pm 3	1.9 \pm 0.7	11	$D = 0.58$ $p = 0.01$
GTP- γ -S	GTP- γ -S	2.1 \pm 0.6	0.51 \pm 0.1	21	$D = 0.22$ $p = 0.67$
GTP- γ -S	50 μ M Taxol	2.1 \pm 0.5	0.51 \pm 0.1	32	$D = 0.23$ $p = 0.50$
GTP	Copolymerized with 1:100 tau; 50 μ M Taxol; tau added post at 1:1	15 \pm 4	4 \pm 1	38	$D = 0.68$ $p = 5 \times 10^{-6}$
GTP	50 μ M Taxol; tau added post at 1:1	2.0 \pm 0.3	0.49 \pm 0.07	50	$D = 0.20$ $p = 0.61$
GTP	50 μ M Taxol; MAP4 added post at 1:2	2.2 \pm 0.4	0.6 \pm 0.1	22	$D = 0.3$ $p = 0.29$

experimental studies that demonstrated a length-dependent persistence length (6,42) used an assay in which only one end was free to fluctuate. This may enable visualization of mechanical modes of shearing between protofilaments that are inaccessible when the entire filament is free to fluctuate.

We and others have proposed that Taxol stabilizes microtubules precisely because it enhances the flexibility of the bonds between dimers (7,43). Increased flexibility imparted by Taxol relieves the internal stress on each dimer. Dimers with GDP in the exchangeable site (E-site) of the β -tubulin have the lowest energy state of a bent-back conformation, but it is being forced straight by the neighboring protofilaments. This competition of conformations in the body of the microtubule filament encourages dynamic instability. Because Taxol increases the flexibility of the interdimer bonds, it enables some of the stress to be relieved, effectively inhibiting dynamic instability and stabilizing the filament. Thus, although Taxol inhibits dynamic instability it also makes microtubules more flexible as a whole.

We also measured the effects of doubly stabilized microtubules to determine whether the increased stiffness of GMPCPP microtubules can dominate the flexibility imparted by Taxol. We find that the stiffening ability of GMPCPP in the nucleotide pocket dominates over the enhanced flexibility afforded by Taxol binding. Vale et al. phenomenologically demonstrated this effect during gliding assay analysis of curvatures, where kinesin motors adhered to a surface drove microtubule gliding (44). Although we use far less Taxol (50 μ M) compared to GMPCPP (1 mM) in our assays, given the known binding affinity of Taxol for GMPCPP microtubules ($K_D = 15$ nM) (45,46), we believe we are saturating our microtubules with Taxol in every binding pocket. Thus, we do not believe that these results are due to an absence of Taxol along the microtubule.

It is perhaps not surprising that GMPCPP dominate over Taxol's effects, considering the structural differences in microtubules in the presence of these two stabilizers. Meurer-Grob et al. used cryo-electron microscopy and helical reconstruction to show that GMPCPP microtubules and Taxotere-stabilized microtubules have different lateral and interprotofilament associations (47). GMPCPP in the E-site of the β -tubulin enhances lateral and longitudinal contacts. Hydrolysis of GTP in the E-site reduces the interdimer interactions, especially the lateral ones, resulting in fewer interprotofilament lateral interactions in GDP-Taxol microtubules compared to GMPCPP microtubules. A recent study of microtubules with 8.8 Å resolution compared GDP-Taxol and GMPCPP microtubules and showed that GMPCPP microtubules make additional contact between helix 3 and helix 9 in the β -tubulin (48). Further, several studies have demonstrated that the protofilaments of GMPCPP microtubules are straighter than those of unstabilized or Taxol-stabilized protofilaments after cold and calcium-induced depolymerization (49,50). Since GMPCPP dimers are in a straight conformation, there are likely increased lateral interactions between protofilaments, and we would expect this to dominate over Taxol-induced flexibility.

GTP- γ -S makes microtubules more flexible, like Taxol

GTP- γ -S is a nonhydrolyzable analog of GTP that is a poor nucleator of microtubules from tubulin dimers without MAPs or Taxol (51). A recent result showed that despite its inability to nucleate microtubules, GTP- γ -S can polymerize microtubules from GMPCPP seeds and that it acts as a better substrate for the binding of EB proteins (11). In our experiments, we found that Taxol was required to polymerize and stabilize microtubules polymerized in the presence of GTP- γ -S, consistent with previous reports.

We found that GTP- γ -S microtubules were still stable after washing out Taxol, like GMPCPP microtubules (Fig. S2 A). Unlike GMPCPP microtubules, GTP- γ -S microtubules were not cold-stable (Fig. S2 B). To test the mechanical properties of GTP- γ -S microtubules with and without Taxol, we created microtubules polymerized in the presence of GTP- γ -S and Taxol. After polymerization, one set of microtubules was washed, with two rounds of pelleting the microtubules and resuspending in buffer without Taxol. The other set was pelleted and resuspended with buffer in the presence of Taxol.

We measured the persistence length of GTP- γ -S microtubules with and without Taxol. We found the average to be 0.51 ± 0.1 mm for GTP- γ -S both with and without Taxol (Table 1). These two data sets showed no statistical difference, indicating that the presence or absence of Taxol does not alter the mechanical properties of GTP- γ -S microtubules. We similarly conclude that GTP- γ -S microtubules are identical to Taxol microtubules when comparing the log-transformed distributions with the Student's t -test ($p = 0.49$ for GTP- γ -S and 0.53 for GTP- γ -S with Taxol) or the K-S test ($p = 0.67$ for GTP- γ -S and 0.50 for GTP- γ -S with Taxol).

The flexibility of GTP- γ -S microtubules after Taxol washout was as flexible as Taxol microtubules with GDP in the β -tubulin E-site (Fig. 2). Thus, our data reveal that GTP- γ -S is the second stabilizer that makes microtubules more flexible, like Taxol. It is interesting that GTP- γ -S has the opposite effect from GMPCPP, since they are both GTP-mimicking analogs. Further, a recent structural study that examined the structure of GDP and GTP- γ -S microtubules at 8.2 Å resolution found that, similar to GMPCPP microtubules, GTP- γ -S microtubules have more contacts between protofilaments than do GDP-Taxol microtubules (52). In particular, both studies find an enhanced interaction between helices 3 and 9 on the β -tubulin (48,52). Thus, GTP- γ -S and GMPCPP microtubules have similarly enhanced side-to-side interactions, but GMPCPP increases stiffness, whereas GTP- γ -S increases flexibility. How might GMPCPP stiffen microtubules, whereas GTP- γ -S softens them? One explanation is that there may be an increase in lateral interactions in GTP- γ -S microtubules compared to GDP microtubules, but their number might still be less than that for GMPCPP microtubules. Another possibility is that GTP- γ -S does not straighten the protofilaments of microtubules as GMPCPP does. No study has examined protofilaments of GTP- γ -S microtubules, but if they are curved, in a GDP-like conformation, that could explain the poor nucleating ability of GTP- γ -S and the requirement of Taxol to form microtubules. Further, if GTP- γ -S microtubule protofilaments were curved, resulting in more flexible microtubules, it would imply that longitudinal interactions between dimers are more important than lateral interactions in determining the mechanical properties of microtubules.

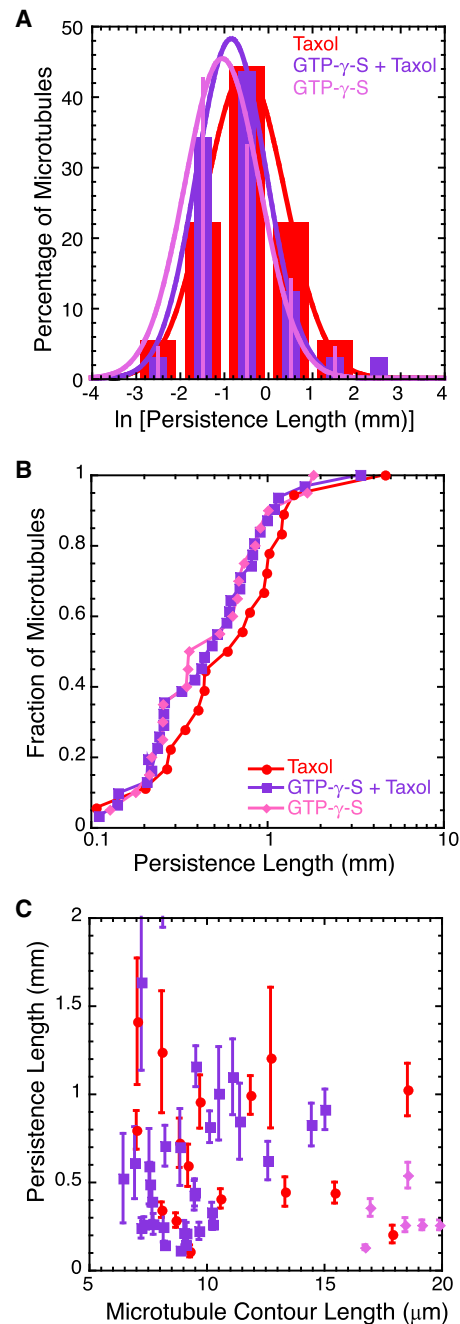


FIGURE 2 GTP- γ -S makes microtubules more flexible. (A) Histograms of data after log-transforming the persistence length show no difference between Taxol-stabilized microtubules (red bars) and microtubules polymerized in the presence of GTP- γ -S with Taxol (purple bars) and without Taxol present (magenta bars). We fit the data to Gaussian functions (Eq. 2); fit parameters are given in Table S1. (B) Normalized cumulative distributions of persistence length for Taxol-stabilized microtubules (red circles) and microtubules polymerized in the presence of GTP- γ -S with Taxol (purple squares) or without Taxol (magenta diamonds) show overlapping distributions, with a slight shift toward lower persistence lengths for both GTP- γ -S microtubule data. (C) We see no length dependence of the persistence lengths for Taxol-stabilized microtubules (red circles) or for microtubules polymerized in the presence of GTP- γ -S with Taxol (purple squares) or without Taxol (magenta diamonds). Error bars represent the mean \pm SE. The numbers of microtubules in each distribution are given in Table 1.

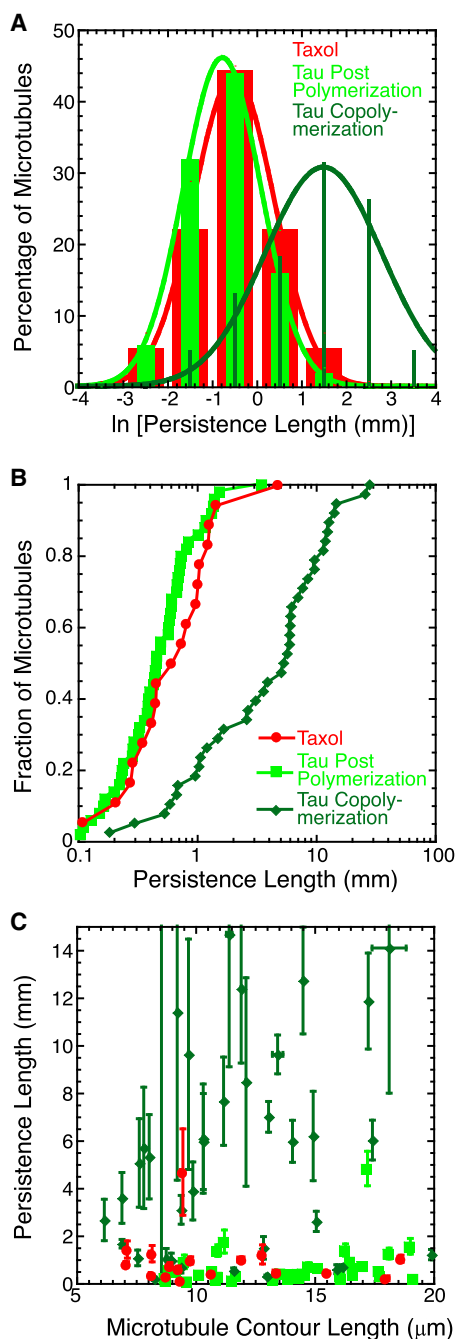


FIGURE 3 Microtubule rigidity increases when polymerized in the presence of tau. (A) Histograms of data after log-transforming the persistence length show that the presence of even 1% tau during polymerization (dark green bars) increased persistence length compared to Taxol-stabilized microtubules (red bars) or Taxol-stabilized microtubules with tau added at 100% after stabilization (light green bars). We fit the data to Gaussian functions (Eq. 2); fit parameters are given in Table S1. (B) Normalized cumulative distributions of persistence length for Taxol-stabilized microtubules (red circles) and Taxol-stabilized microtubules with tau added at 100% after stabilization (light green squares) show overlapping distributions. Conversely, microtubules polymerized in the presence of 1% tau (dark green diamonds) show a distinct distribution shifted far to higher persistence lengths. (C) We see no length dependence of the persistence lengths for Taxol-stabilized microtubules (red circles), Taxol-stabilized

Tau stiffens microtubules, depending on its presence during polymerization

We measured the persistence length of microtubules in the presence of 4RL tau protein, the longest tau isoform. We made microtubules with tau in two ways: 1), tau was included at a 1:100 tau/tubulin molar ratio during polymerization, and microtubules were then further stabilized with saturating Taxol and a tau/tubulin ratio of 1:1 added postpolymerization; or 2), tau was added after polymerization and stabilization with saturating Taxol at a tau/tubulin ratio of 1:1. We found that the order in which tau was added had differential effects on microtubule rigidity. As above, we compared the results to our control data set of microtubules stabilized with Taxol alone.

For microtubules to which tau was added after polymerization and Taxol stabilization, little difference was found when compared to the Taxol-stabilized microtubule control data set, as can be seen in the log-transformed data and the cumulative distributions (Fig. 3, A and B). Both displayed log-normal distributions. Further, the average persistence length for microtubules with tau added after polymerization was 0.49 ± 0.07 mm, which is similar to that for Taxol-stabilized microtubules, which had an average persistence length of 0.6 ± 0.1 mm (Table 1). We compared the two data sets using Student's *t*-test on the log-transformed histograms (Fig. 3 A) and found no evidence of a difference ($p = 0.35$). We also used the K-S test on normalized cumulative distributions (Fig. 3 B) and found no evident divergence ($D = 0.20$ and p -value = 0.61). Thus, we conclude that adding tau after polymerization and stabilization with Taxol does not affect the mechanical rigidity of microtubules.

When tau was included during polymerization and before stabilization with Taxol, we found a large difference in both the distribution and average persistence length compared to Taxol-stabilized microtubules alone or those with tau added after polymerization (Fig. 3, A and B). Tau's presence during polymerization causes an increase in the average persistence length to 4 ± 1 mm (Table 1). We found, by comparing the log-transformed histograms (Fig. 3 A) and performing Student's *t*-tests, that the probability that these distributions are the same is $<0.01\%$ ($p < 0.0001$). K-S statistical comparisons of normalized cumulative distributions (Fig. 3 B) between the data sets of microtubules polymerized with tau and those polymerized without tau showed that these distributions have no likelihood of being the same ($D = 0.68$ and $p = 5 \times 10^{-6}$). Interestingly, the statistics of the distribution show a relatively low probability ($p = 0.14$) that the data is log-normal (Fig. S3). Further, we found that

microtubules with tau added at 100% after stabilization (light green squares), nor for microtubules polymerized in the presence of 1% tau (dark green diamonds). Error bars represent standard error of the mean. The numbers of microtubules in each distribution are given in Table 1.

the persistence length is independent of contour length for all data sets (Fig. 3 C).

Our results indicate that the ability of tau to affect the mechanical properties of microtubules differs depending on when the tau binds to the microtubules—during or after polymerization. We find that when it is added during polymerization, tau has a substantial effect on microtubule rigidity, increasing it by a factor of 4, even when added at a low 1:100 molar ratio with tubulin. These microtubules were further stabilized with Taxol, but the addition of Taxol had little effect on the rigidity. Thus, when tau is present during polymerization, its ability to mechanically stiffen microtubules dominates over Taxol's effect of increasing microtubule flexibility. On the other hand, when Taxol is added first, its effect on the mechanical properties of microtubules is dominant.

There are two possible explanations for these effects that have been proposed in the literature: 1), Taxol and tau could be competing for the same interior binding site of microtubules on the β -tubulin (22); or 2), Taxol and tau bind to locations on opposite sides of the tubulin dimer, but each causes conformational changes that disallow the binding of the other (53). In either scenario, the binding of one inhibits the binding of the other resulting in differential effects on the mechanical properties of microtubules, which is consistent with our results.

There is biochemical and structural evidence that tau and Taxol compete for the same binding site on the luminal side of the β -tubulin when tau is present during polymerization (22). Further, several biochemical studies have demonstrated that tau can bind to microtubules by two distinct modes, presumably at two different binding sites that have different affinities (54–57). At least one site for tau binding exists on the exterior of microtubules, since it has been demonstrated that tau can bind to preformed microtubules (37,58,59) and such binding has been imaged by atomic force microscopy *in vitro* (60,61) and electron microscopy in cells (12) and *in vitro* (62,63). The second site it could bind to is the microtubule lumen or another exterior site. If the second site is in the microtubule lumen, it is unlikely for this site to be accessible by tau after polymerization, since the radius of gyration for full-length tau (441 amino acids that are each ~ 0.5 nm in length) is 6.5 nm (64). This is similar to the interior radius of the microtubule, which is ~ 8.5 nm (65), and would entropically inhibit the entrance of tau into the lumen after polymerization. Thus, if there is an interior tau-binding site, it should only be accessible during polymerization or in cases of high osmotic pressure (66).

Previous studies have measured the effects of tau and other MAPs on the rigidity of microtubules. Mickey et al. added tau to microtubules at a 20:1 tau/tubulin ratio after polymerization and found the same rigidity as for microtubules with Taxol (7.5–7.9 mm) (9). Despite the much larger persistence length in that study compared to our measure-

ments, both studies found that tau added after polymerization results in the same rigidity as Taxol stabilization alone. A second study used a forced oscillatory motion by an optical tweezers to measure the effects of Taxol and added tau on microtubule rigidity (4). They found that Taxol decreased the rigidity of microtubules from 0.9 mm to 0.2 mm, similar to our measured values. They tested the effects of adding tau to microtubules after polymerization at varying tau/tubulin ratios (2:100 to 85:100) without Taxol. Even at these high concentrations, they still only found a twofold increase in persistence length (maximum of 2.5 mm), most likely because they added the tau after polymerization.

Interestingly, our study is, to our knowledge, the only study of microtubule mechanical properties that has added tau during polymerization. The effect of tau copolymerization was much stronger than that of adding tau at saturating concentrations postpolymerization, and it overpowered the effect of Taxol binding. Our results are consistent with the view that there is a competition between tau and Taxol for an interior binding site, and they suggest that binding to the Taxol site has a large effect on the rigidity of microtubules. Further, the effect is large even at very low concentrations of tau added during polymerization. This is important, because tau is present during the polymerization of microtubules in cells, and it is not at saturating concentrations. Thus, microtubules of the axon are likely to be far stiffer than normal microtubules, which are needed to support the long, extended structure of nerves.

MAP4 alters the distribution in persistence length

We measured the mechanical properties of microtubules in the presence of MAP4 to compare the results to those with tau. MAP4 is often described as analogous to tau, except that it is confined to the cell body and expressed ubiquitously in multiple tissues. Despite their sequence similarities, we find that MAP4 is very different from tau in its nucleation, stabilization, and mechanical-stiffening abilities. First, we noticed that MAP4 was unable to nucleate microtubules when added during polymerization of tubulin at 37°C. Even after adding Taxol, few microtubules were formed, and most were too short to perform the mechanical analysis. Instead, we polymerized microtubules without Taxol, stabilized with Taxol, and with MAP4 added at a 1:2 MAP4/tubulin molar ratio. This process resulted in many well-formed microtubules in the length range we are accustomed to measuring. By examining a GFP-labeled MAP4 in two-color fluorescence, we determined that MAP4 was able to bind and bundle microtubules (Fig. 4 A).

We found that the average persistence length of microtubules with MAP4 was 0.5 ± 0.1 mm, which is similar to the persistence length of Taxol-stabilized microtubules of 0.6 ± 0.1 mm (Table 1). Despite these similar average persistence lengths, we find that the distribution of

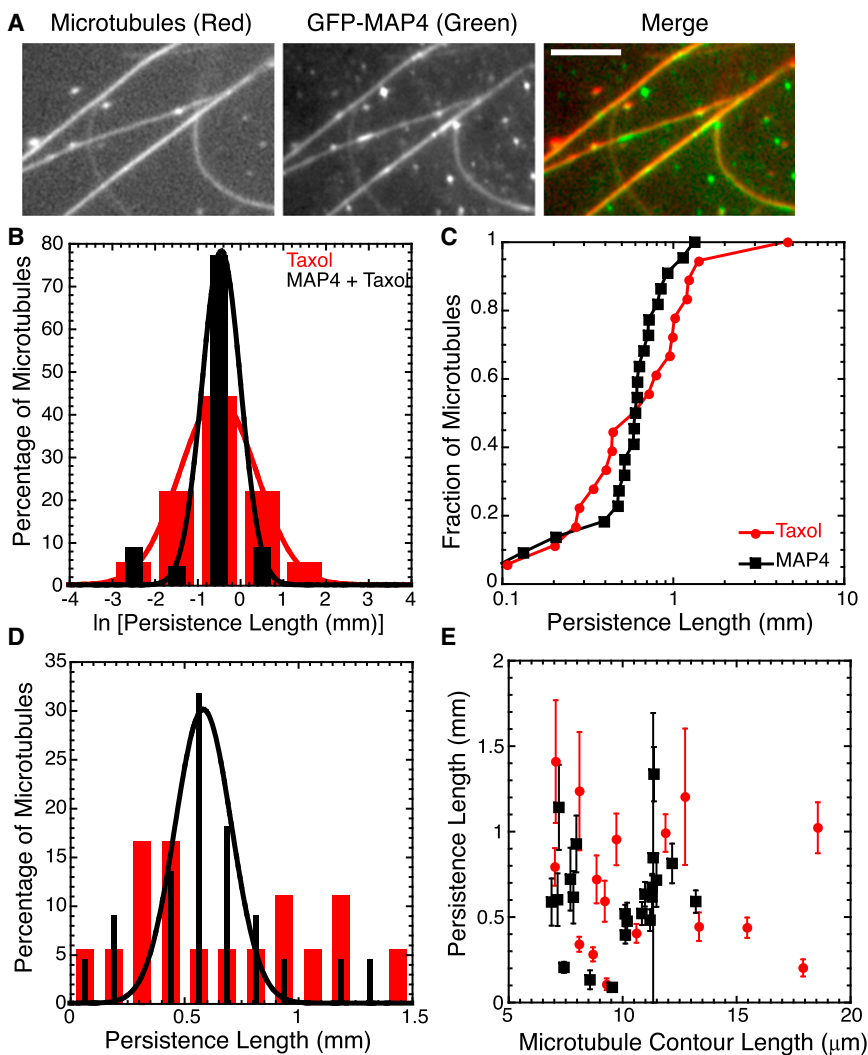


FIGURE 4 MAP4 reduces the distribution width of Taxol-stabilized microtubules. (A) GFP-oMAP4 bound and bundled microtubules at the concentrations used in our studies. (B) Histograms of data after log-transforming the persistence length show a wider distribution for Taxol-stabilized microtubules (red bars) compared to Taxol-stabilized microtubules in the presence of MAP4 (black bars). We fit the data to Gaussian functions (Eq. 2); fit parameters are given in Table S1. (C) Normalized cumulative distributions of persistence length for Taxol-stabilized microtubules (red circles) and Taxol-stabilized microtubules in the presence of MAP4 (black squares) show overlapping distributions, but the sigmoidal shape of the MAP4 data is a clear signature of a normal Gaussian distribution. (D) Histograms comparing microtubule persistence lengths polymerized and then stabilized with Taxol (red bars) with persistence length of microtubules polymerized then stabilized with Taxol with MAP4 added postpolymerization at a 1:2 ratio (black bars). The distributions are clearly distinct. The Taxol-stabilized microtubule distribution of persistence lengths is consistent with a log-normal distribution. The persistence-length distribution of Taxol-stabilized microtubules with MAP4 added is consistent with the normal Gaussian distribution. We fit the MAP4 data to a Gaussian function (Eq. 2); fit parameters are given in Table S1. (E) We see no length dependence of the persistence lengths for Taxol-stabilized microtubules (red circles) or for Taxol-stabilized microtubules in the presence of MAP4 (black squares). Error bars represent standard error of the mean. The numbers of microtubules in each distribution are given in Table 1.

persistence lengths with MAP4 appears to be distinct from that of Taxol-stabilized microtubules (Fig. 4, B–D). Comparing the log-transformed and binned data, it is clear that the width of the distribution for the MAP4 data (0.45 ± 0.05) is half that of the data with Taxol only (0.90 ± 0.03) (Fig. 4 B). Further, the signature of a Gaussian distribution in the cumulative representation is a sigmoidal shape, which is clearly shown for the MAP4 data but not the Taxol-alone data (Fig. 4 C).

MAP4-labeled microtubules displayed a symmetric distribution (Fig. 4 D) and was statistically consistent with a normal Gaussian distribution ($p = 0.41$) and not with a log-normal distribution ($p = 0.04$). The differences in distribution shapes are clearly distinguishable by eye in a histogram of binned persistence lengths (Fig. 4 D). When fitting a Gaussian to the data with MAP4, the best fit has a mean value of 0.30 ± 0.04 mm, with a goodness of fit of 0.80. When a Gaussian is fit to the data with Taxol only, the best fit has a mean value of 0.5 ± 0.3 with a goodness of fit of 0.18 (Table S2).

Although the sequence similarity between the microtubule-binding regions of MAP4 and tau or MAP2 is strong, there is no biological basis to think that MAP4 should have the same nucleation, polymerization, stabilization, or stiffening abilities as tau. This is because the microtubules of the neuronal cell body or those of other cell types should not be too stable or too stiff. If MAP4 stiffened or stabilized in the same manner as tau, microtubules would likely overgrow, bundle, and perhaps create processes, as has been shown for tau overexpression in a variety of cell types (14,16). Alternatively, given the requirements of the microtubule network in cell bodies, MAP4 should act to modulate dynamics or stabilize against known destabilizers, such as katanin or kinesin-13s, to regulate microtubule dynamics. Indeed, we know that MAP4 stabilizes microtubules against katanin-induced severing (23) and can regulate dynein attachment to astral microtubules in mitosis (33).

We have demonstrated that MAP4 can alter the distribution of the persistence length of Taxol-stabilized microtubules—collapsing the log-normal distribution into a normal

distribution. Some possible mechanisms for this are that 1), MAP4 reduces the variance in the Young's modulus (E) of the microtubules, or 2), MAP4 reduces the variance in the second moment of area (I) of the microtubules. A product of these two properties, EI , is proportional to the persistence length we measure:

$$L_p = \frac{EI}{k_B T}, \quad (3)$$

where k_B is Boltzmann's constant and T is the temperature.

For the first mechanism, it is possible that MAP4 binding to the microtubule could reduce the variance in the Young's modulus so that all the microtubules have the same material stiffness, E . If this occurred, the Gaussian distribution in persistence lengths would come solely from the normal distribution in the second moment of area, I , which depends on the fourth power of the cross-sectional radius of microtubules. Thus, the differences in protofilament number that change the radius are likely to result in a distribution of the second moments of area between microtubules of a population. Even within one microtubule, the cross-sectional area changes frequently. It has been estimated by electron microscopy measurements using the moiré patterns between the top and bottom of the microtubule that Taxol microtubules have defects every 10–15 μm (67). These measurements are insensitive to fast transitions in protofilament number because a minimum length is required to determine the moiré pattern. Theoretical deductions based on katanin severing activities estimate the frequency of defects along the length of microtubules closer to once per 0.6 μm (68), spreading the variance in the second moment of inertia even more. Finally, recent experiments showed that doublecortin protein binds with high affinity to microtubules with 13 protofilaments, but with lower affinity to microtubules with other numbers of protofilament (69). Images from this study show that Taxol microtubules have multiple short transitions in protofilament number.

In the second mechanism, MAP4 would lower the variance in the second moment of the area, I . If this occurred, then the Gaussian distribution in persistence lengths would come from a normal distribution in the Young's modulus, or material stiffness, E . Although it seems unlikely that the binding of MAP4 could change the second moment of area of a preformed microtubule, so as to collapse the distribution, there is evidence for these types of manipulations. For instance, small-angle x-ray scattering (SAXS) experiments have reported the alteration of the microtubule cross-sectional area during the addition of Taxol and MAPs (70–73). If MAP4 binding were able to create a population of microtubules in which all have the same cross-sectional radius, then the variance in the persistence-length distribution would come from differences in the Young's modulus alone. This is a possible mechanism that cannot be ruled out based on our data.

CONCLUSION

We find that adding multiple stabilizing agents does not result in cumulative effects on microtubule mechanics. To the contrary, we find that one type of stabilizer tends to dominate the mechanical properties. In particular, we found that GMPCPP is a potent mechanical stabilizer and its stiffening effect dominates over Taxol's ability to mechanically weaken the microtubule filament. Further, the stiffening effects of tau were dominant over Taxol's effects when tau was added during polymerization, but tau was ineffective when added postpolymerization. Finally, we found that GTP- γ -S makes microtubules more flexible. Alternatively, MAP4 did not change the persistence length of microtubules, but it altered the distribution significantly.

SUPPORTING MATERIAL

Three figures and two tables are available at [http://www.biophysj.org/biophysj/supplemental/S0006-3495\(13\)00243-9](http://www.biophysj.org/biophysj/supplemental/S0006-3495(13)00243-9).

We thank Megan Bailey for the purified tau protein.

T.L.H. was supported in part by a North East Alliance for Graduate Education and Professoriate (NEAGEP) grant from the National Science Foundation (NSF). T.L.H. and D.S. were supported by an NSF grant (No. 1039403) and J.L.R. and D.S. by a supplement (No. 0928540) from the Nano and Bio Mechanics Program, Civil Mechanical, and Manufacturing Innovation Directorate. A.S. is supported by a program grant from Marie Curie Cancer Care.

REFERENCES

1. Dye, R. B., S. P. Fink, and R. C. Williams, Jr. 1993. Taxol-induced flexibility of microtubules and its reversal by MAP-2 and tau. *J. Biol. Chem.* 268:6847–6850.
2. Venier, P., A. C. Maggs, ..., D. Pantaloni. 1994. Analysis of microtubule rigidity using hydrodynamic flow and thermal fluctuations. *J. Biol. Chem.* 269:13353–13360.
3. Felgner, H., R. Frank, and M. Schliwa. 1996. Flexural rigidity of microtubules measured with the use of optical tweezers. *J. Cell Sci.* 109:509–516.
4. Felgner, H., R. Frank, ..., M. Schliwa. 1997. Domains of neuronal microtubule-associated proteins and flexural rigidity of microtubules. *J. Cell Biol.* 138:1067–1075.
5. Kikumoto, M., M. Kurachi, ..., H. Tashiro. 2006. Flexural rigidity of individual microtubules measured by a buckling force with optical traps. *Biophys. J.* 90:1687–1696.
6. Kawaguchi, K., and A. Yamaguchi. 2010. Temperature dependence rigidity of non-taxol stabilized single microtubules. *Biochem. Biophys. Res. Commun.* 402:66–69.
7. Sept, D., and F. C. MacKintosh. 2010. Microtubule elasticity: connecting all-atom simulations with continuum mechanics. *Phys. Rev. Lett.* 104:018101.
8. Hyman, A. A., S. Salser, ..., T. J. Mitchison. 1992. Role of GTP hydrolysis in microtubule dynamics: information from a slowly hydrolyzable analogue, GMPCPP. *Mol. Biol. Cell.* 3:1155–1167.
9. Mickey, B., and J. Howard. 1995. Rigidity of microtubules is increased by stabilizing agents. *J. Cell Biol.* 130:909–917.
10. Varga, V., C. Leduc, ..., J. Howard. 2009. Kinesin-8 motors act cooperatively to mediate length-dependent microtubule depolymerization. *Cell.* 138:1174–1183.

11. Maurer, S. P., P. Bieling, ..., T. Surrey. 2011. GTP γ S microtubules mimic the growing microtubule end structure recognized by end-binding proteins (EBs). *Proc. Natl. Acad. Sci. USA*. 108:3988–3993.
12. Chen, J., Y. Kanai, ..., N. Hirokawa. 1992. Projection domains of MAP2 and tau determine spacings between microtubules in dendrites and axons. *Nature*. 360:674–677.
13. Iqbal, K., F. Liu, ..., I. Grundke-Iqbal. 2009. Mechanisms of tau-induced neurodegeneration. *Acta Neuropathol.* 118:53–69.
14. Kanai, Y., R. Takemura, ..., N. Hirokawa. 1989. Expression of multiple tau isoforms and microtubule bundle formation in fibroblasts transfected with a single tau cDNA. *J. Cell Biol.* 109:1173–1184.
15. Knops, J., K. S. Kosik, ..., L. McConlogue. 1991. Overexpression of tau in a nonneuronal cell induces long cellular processes. *J. Cell Biol.* 114:725–733.
16. Lee, G., and S. L. Rook. 1992. Expression of tau protein in non-neuronal cells: microtubule binding and stabilization. *J. Cell Sci.* 102:227–237.
17. Kanai, Y., J. Chen, and N. Hirokawa. 1992. Microtubule bundling by tau proteins in vivo: analysis of functional domains. *EMBO J.* 11:3953–3961.
18. Brandt, R., and G. Lee. 1993. Functional organization of microtubule-associated protein tau. Identification of regions which affect microtubule growth, nucleation, and bundle formation in vitro. *J. Biol. Chem.* 268:3414–3419.
19. Reference deleted in proof.
20. Brandt, R., and G. Lee. 1994. Orientation, assembly, and stability of microtubule bundles induced by a fragment of tau protein. *Cell Motil. Cytoskeleton.* 28:143–154.
21. Levy, S. F., A. C. Leboeuf, ..., S. C. Feinstein. 2005. Three- and four-repeat tau regulate the dynamic instability of two distinct microtubule subpopulations in qualitatively different manners. Implications for neurodegeneration. *J. Biol. Chem.* 280:13520–13528.
22. Kar, S., J. Fan, ..., L. A. Amos. 2003. Repeat motifs of tau bind to the insides of microtubules in the absence of taxol. *EMBO J.* 22:70–77.
23. McNally, K. P., D. Buster, and F. J. McNally. 2002. Katanin-mediated microtubule severing can be regulated by multiple mechanisms. *Cell Motil. Cytoskeleton.* 53:337–349.
24. Holmfeldt, P., G. Brattsand, and M. Gullberg. 2002. MAP4 counteracts microtubule catastrophe promotion but not tubulin-sequestering activity in intact cells. *Curr. Biol.* 12:1034–1039.
25. Murofushi, H., S. Kotani, ..., H. Sakai. 1986. Purification and characterization of a 190-kD microtubule-associated protein from bovine adrenal cortex. *J. Cell Biol.* 103:1911–1919.
26. Ookata, K., S. Hisanaga, ..., T. Kishimoto. 1995. Cyclin B interaction with microtubule-associated protein 4 (MAP4) targets p34cdc2 kinase to microtubules and is a potential regulator of M-phase microtubule dynamics. *J. Cell Biol.* 128:849–862.
27. West, R. R., K. M. Tenbarge, and J. B. Olmsted. 1991. A model for microtubule-associated protein 4 structure. Domains defined by comparisons of human, mouse, and bovine sequences. *J. Biol. Chem.* 266:21886–21896.
28. Mangan, M. E., and J. B. Olmsted. 1996. A muscle-specific variant of microtubule-associated protein 4 (MAP4) is required in myogenesis. *Development.* 122:771–781.
29. Strausberg, R. L., E. A. Feingold, ..., M. A. Marra; Mammalian Gene Collection Program Team. 2002. Generation and initial analysis of more than 15,000 full-length human and mouse cDNA sequences. *Proc. Natl. Acad. Sci. USA*. 99:16899–16903.
30. Ota, T., Y. Suzuki, ..., S. Sugano. 2004. Complete sequencing and characterization of 21,243 full-length human cDNAs. *Nat. Genet.* 36:40–45.
31. Chapin, S. J., C. M. Lue, ..., J. C. Bulinski. 1995. Differential expression of alternatively spliced forms of MAP4: a repertoire of structurally different microtubule-binding domains. *Biochemistry.* 34:2289–2301.
32. Tokuraku, K., T. Q. Noguchi, ..., S. Kotani. 2007. An isoform of microtubule-associated protein 4 inhibits kinesin-driven microtubule gliding. *J. Biochem.* 141:585–591.
33. Samora, C. P., B. Mogessie, ..., A. D. McAinsh. 2011. MAP4 and CLASP1 operate as a safety mechanism to maintain a stable spindle position in mitosis. *Nat. Cell Biol.* 13:1040–1050.
34. Hawkins, T. L., M. Mirigian, ..., J. L. Ross. 2012. Perturbations in microtubule mechanics from tubulin preparation. *Cell. Mol. Bioeng.* 5:227–238.
35. Gittes, F., B. Mickey, ..., J. Howard. 1993. Flexural rigidity of microtubules and actin filaments measured from thermal fluctuations in shape. *J. Cell Biol.* 120:923–934.
36. Peloquin, J., Y. Komarova, and G. Borisy. 2005. Conjugation of fluorophores to tubulin. *Nat. Methods.* 2:299–303.
37. Ross, J. L., C. D. Santangelo, ..., D. K. Fygenson. 2004. Tau induces cooperative Taxol binding to microtubules. *Proc. Natl. Acad. Sci. USA*. 101:12910–12915.
38. Dixit, R., J. L. Ross, ..., E. L. Holzbaur. 2008. Differential regulation of dynein and kinesin motor proteins by tau. *Science*. 319:1086–1089.
39. Reference deleted in proof.
40. Kirkman, T. W. Statistics to Use. <http://www.physics.csbsju.edu/stats/>.
41. R Development Code Team. 2011. R: A Language and Environment for Statistical Computing. R Foundation for Statistical Computing, Vienna, Austria.
42. Pampaloni, F., G. Lattanzi, ..., E. L. Florin. 2006. Thermal fluctuations of grafted microtubules provide evidence of a length-dependent persistence length. *Proc. Natl. Acad. Sci. USA*. 103:10248–10253.
43. Mitra, A., and D. Sept. 2008. Taxol allosterically alters the dynamics of the tubulin dimer and increases the flexibility of microtubules. *Biophys. J.* 95:3252–3258.
44. Vale, R. D., C. M. Coppin, ..., R. A. Milligan. 1994. Tubulin GTP hydrolysis influences the structure, mechanical properties, and kinesin-driven transport of microtubules. *J. Biol. Chem.* 269:23769–23775.
45. Li, Y., R. Edsall, Jr., ..., S. Bane. 2000. Equilibrium studies of a fluorescent paclitaxel derivative binding to microtubules. *Biochemistry.* 39:616–623.
46. Ross, J. L., and D. K. Fygenson. 2003. Mobility of taxol in microtubule bundles. *Biophys. J.* 84:3959–3967.
47. Meurer-Grob, P., J. Kasparian, and R. H. Wade. 2001. Microtubule structure at improved resolution. *Biochemistry.* 40:8000–8008.
48. Yajima, H., T. Ogura, ..., N. Hirokawa. 2012. Conformational changes in tubulin in GMPCPP and GDP-taxol microtubules observed by cryo-electron microscopy. *J. Cell Biol.* 198:315–322.
49. Müller-Reichert, T., D. Chrétien, ..., A. A. Hyman. 1998. Structural changes at microtubule ends accompanying GTP hydrolysis: information from a slowly hydrolyzable analogue of GTP, guanylyl (α,β)methylene-diphosphonate. *Proc. Natl. Acad. Sci. USA*. 95:3661–3666.
50. Elie-Caille, C., F. Severin, ..., A. A. Hyman. 2007. Straight GDP-tubulin protofilaments form in the presence of taxol. *Curr. Biol.* 17:1765–1770.
51. Hamel, E., and C. M. Lin. 1984. Guanosine 5'-O-(3-thiotriphosphate), a potent nucleotide inhibitor of microtubule assembly. *J. Biol. Chem.* 259:11060–11069.
52. Maurer, S. P., F. J. Fourniol, ..., T. Surrey. 2012. EBs recognize a nucleotide-dependent structural cap at growing microtubule ends. *Cell.* 149:371–382.
53. Preuss, U., J. Biernat, ..., E. Mandelkow. 1997. The 'jaws' model of tau-microtubule interaction examined in CHO cells. *J. Cell Sci.* 110:789–800.
54. Chau, M. F., M. J. Radeke, ..., S. C. Feinstein. 1998. The microtubule-associated protein tau cross-links to two distinct sites on each α and β tubulin monomer via separate domains. *Biochemistry.* 37:17692–17703.

55. Makrides, V., M. R. Massie, ..., J. Lew. 2004. Evidence for two distinct binding sites for tau on microtubules. *Proc. Natl. Acad. Sci. USA*. 101:6746–6751.
56. Devred, F., P. Barbier, ..., V. Peyrot. 2004. Tau induces ring and microtubule formation from $\alpha\beta$ -tubulin dimers under nonassembly conditions. *Biochemistry*. 43:10520–10531.
57. Tsvetkov, P. O., A. A. Makarov, ..., F. Devred. 2012. New insights into tau-microtubules interaction revealed by isothermal titration calorimetry. *Biochimie*. 94:916–919.
58. Goode, B. L., and S. C. Feinstein. 1994. Identification of a novel microtubule binding and assembly domain in the developmentally regulated inter-repeat region of tau. *J. Cell Biol.* 124:769–782.
59. Goode, B. L., M. Chau, ..., S. C. Feinstein. 2000. Structural and functional differences between 3-repeat and 4-repeat tau isoforms. Implications for normal tau function and the onset of neurodegenerative disease. *J. Biol. Chem.* 275:38182–38189.
60. Makrides, V., T. E. Shen, ..., S. C. Feinstein. 2003. Microtubule-dependent oligomerization of tau. Implications for physiological tau function and tauopathies. *J. Biol. Chem.* 278:33298–33304.
61. Schaap, I. A., B. Hoffmann, ..., C. F. Schmidt. 2007. Tau protein binding forms a 1 nm thick layer along protofilaments without affecting the radial elasticity of microtubules. *J. Struct. Biol.* 158:282–292.
62. Al-Bassam, J., R. S. Ozer, ..., R. A. Milligan. 2002. MAP2 and tau bind longitudinally along the outer ridges of microtubule protofilaments. *J. Cell Biol.* 157:1187–1196.
63. Santarella, R. A., G. Skiniotis, ..., A. Hoenger. 2004. Surface-decoration of microtubules by human tau. *J. Mol. Biol.* 339:539–553.
64. Mylonas, E., A. Hascher, ..., D. I. Svergun. 2008. Domain conformation of tau protein studied by solution small-angle x-ray scattering. *Biochemistry*. 47:10345–10353.
65. Reference deleted in proof.
66. Needleman, D. J., M. A. Ojeda-Lopez, ..., C. R. Safinya. 2005. Radial compression of microtubules and the mechanism of action of taxol and associated proteins. *Biophys. J.* 89:3410–3423.
67. Arnal, I., and R. H. Wade. 1995. How does taxol stabilize microtubules? *Curr. Biol.* 5:900–908.
68. Davis, L. J., D. J. Odde, ..., S. P. Gross. 2002. The importance of lattice defects in katanin-mediated microtubule severing in vitro. *Biophys. J.* 82:2916–2927.
69. Bechstedt, S., and G. J. Brouhard. 2012. Doublecortin recognizes the 13-protofilament microtubule cooperatively and tracks microtubule ends. *Dev. Cell.* 23:181–192.
70. Díaz, J. F., J. M. Valpuesta, ..., J. M. Andreu. 1998. Changes in microtubule protofilament number induced by Taxol binding to an easily accessible site. Internal microtubule dynamics. *J. Biol. Chem.* 273:33803–33810.
71. Sackett, D. L., V. Chernomordik, ..., R. Nossal. 2003. Use of small-angle neutron scattering to study tubulin polymers. *Biomacromolecules*. 4:461–467.
72. Raviv, U., T. Nguyen, ..., C. R. Safinya. 2007. Microtubule protofilament number is modulated in a stepwise fashion by the charge density of an enveloping layer. *Biophys. J.* 92:278–287.
73. Choi, M. C., U. Raviv, ..., C. R. Safinya. 2009. Human microtubule-associated-protein tau regulates the number of protofilaments in microtubules: a synchrotron x-ray scattering study. *Biophys. J.* 97:519–527.

Mechanical Properties of Doubly Stabilized Microtubule Filaments

Taviare L. Hawkins,^{†‡} David Sept,[§] Binyam Mogessie,[¶] Anne Straube,[¶] and Jennifer L. Ross^{†*}

[†]Department of Physics, University of Massachusetts Amherst, Amherst, Massachusetts; [‡]Department of Physics, University of Wisconsin-La Crosse, La Crosse, Wisconsin; [§]Department of Biomedical Engineering, University of Michigan, Ann Arbor, Michigan; and [¶]Centre for Mechanochemical Cell Biology, Warwick Medical School, University of Warwick, Coventry, United Kingdom

Hawkins et al.

Double-Stable Microtubule Mechanics

*Correspondence: rossj@physics.umass.edu

Binyam Mogessie's present address is MRC Laboratory of Molecular Biology, Cambridge, United Kingdom.

Submitted July 15, 2015, and accepted for publication February 19, 2013.

SUPPLEMENTAL FIGURE CAPTIONS

Supplemental Figure 1. Persistence length does not depend on the contour length of the filament. Persistence length as a function of filament contour length for data taken on microtubules (A) with Taxol only, (B) with GMPCPP, (C) with GMPCPP with Taxol, (E) GTP-g-S, (F) GTP-g-S with Taxol, (G) MAP4 with Taxol, (H) polymerized with tau, and (I) with tau added after Taxol. We have plotted each data set separately on different axes to show that none of our data has a length-dependent persistence length. We fit each data set to a linear function of the form: $y = mx + b$. (D) The fit parameter of the slope with the error of the fit for each data set.

Supplemental Figure 2. GTP- γ -S microtubules are stable to dilution of Taxol and tubulin, but not cold stable. We compared the ability of GTP- γ -S to stabilize microtubules after depletion of tubulin and Taxol or after incubation at 4°C using a flow chamber. Rhodamine-labeled microtubules were polymerized with GMPCPP, GTP- γ -S, or GTP, and then stabilized with 5 μ M Taxol. They were attached to the cover slip of a flow chamber using rigor mutant kinesin (kinesin-560 T99N), washed with PEM-100 with 5 μ M Taxol to remove unbound filaments, and imaged with an EM-CCD camera (“With Taxol”). All chambers showed microtubules. As previously reported, the GMPCPP microtubules were shorter than the GTP or GTP- γ -S microtubules because GMPCPP nucleates microtubules quickly.

Next, 15 chamber volumes of PEM-100 without Taxol was flowed into the chamber, and the filaments were imaged again (“Taxol Wash Out”). The GMPCPP microtubules were still bound at high concentration. The GTP microtubules were obviously shorter and fewer in the chamber. The GTP- γ -S microtubules still appeared long with as many microtubules as prior to the washout.

Finally, the flow chambers were incubated at 4°C for 10 minutes and imaged again. The GMPCPP microtubules were bound with high concentration of filaments. The GTP microtubules

were completely gone from the chamber. The GTP- γ -S microtubules were obviously shorter with fewer microtubules bound to the cover glass.

The scale bar represented 10 μm , and is the same for all images.

Supplemental Figure 3. Histogram of microtubule persistence lengths for microtubules polymerized in the presence of tau at 1:100 and subsequently stabilized with Taxol and tau at 1:1. The distribution is inconsistent with a normal, Gaussian distribution ($D = 0.68$, $p = 2.2 \times 10^{-16}$). It is also inconsistent with a log-normal distribution ($D = 0.51$, $p = 7.7 \times 10^{-10}$).

Supplemental Table 1. Parameters for Gaussian fits of Log-transformed histograms.

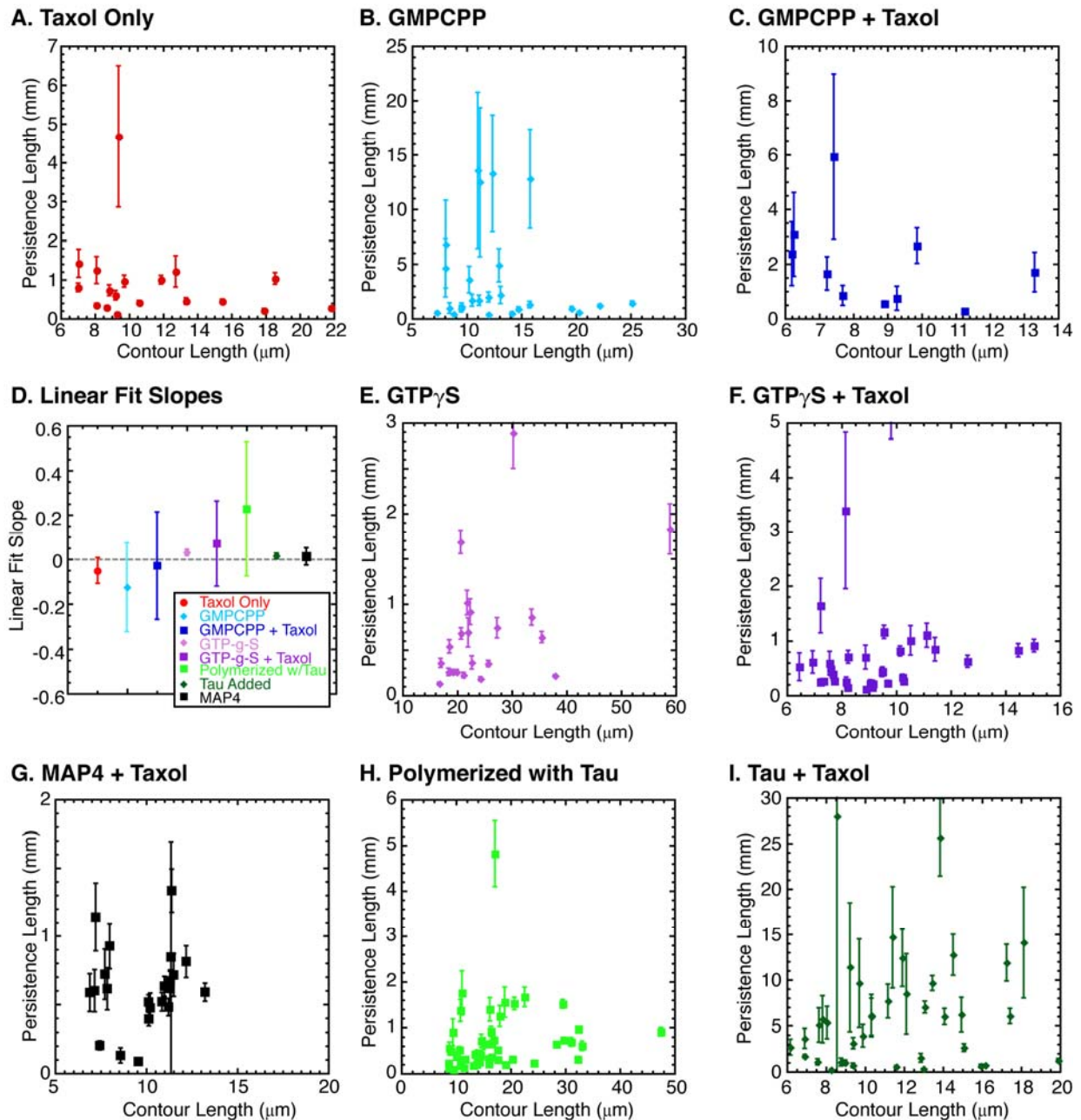
Data Set	Amplitude, A	Mean, x_0	Standard Deviation, σ	Goodness of fit, R^2
Taxol	43 ± 1	-0.50 ± 0.03	0.90 ± 0.03	0.99
GMPCPP	34 ± 5	0.3 ± 0.2	1.2 ± 0.2	0.85
GMPCPP+Taxol	37 ± 4	0.3 ± 0.1	1.0 ± 0.1	0.93
GTP- γ -S	48 ± 5	-1.02 ± 0.1	0.9 ± 0.1	0.94
GTP- γ -S+Taxol	48 ± 2	-0.82 ± 0.04	0.79 ± 0.04	0.99
Tau Added Before Polymerization	31 ± 3	1.5 ± 0.2	1.3 ± 0.2	0.93
Tau Added After Polymerization	46 ± 0.2	-0.76 ± 0.01	0.87 ± 0.01	1.00
MAP4+Taxol	78 ± 5	-0.43 ± 0.05	0.45 ± 0.05	0.98

Supplemental Table 2. Parameters for Gaussian fits of histogram for MAP4.

Data Set	Amplitude, A	Mean, x_0	Standard Deviation, σ	Goodness of fit, R^2
Taxol	10 ± 2	0.49 ± 0.29	0.66 ± 0.37	0.18
MAP4+Taxol	30 ± 4	0.59 ± 0.02	0.12 ± 0.02	0.79

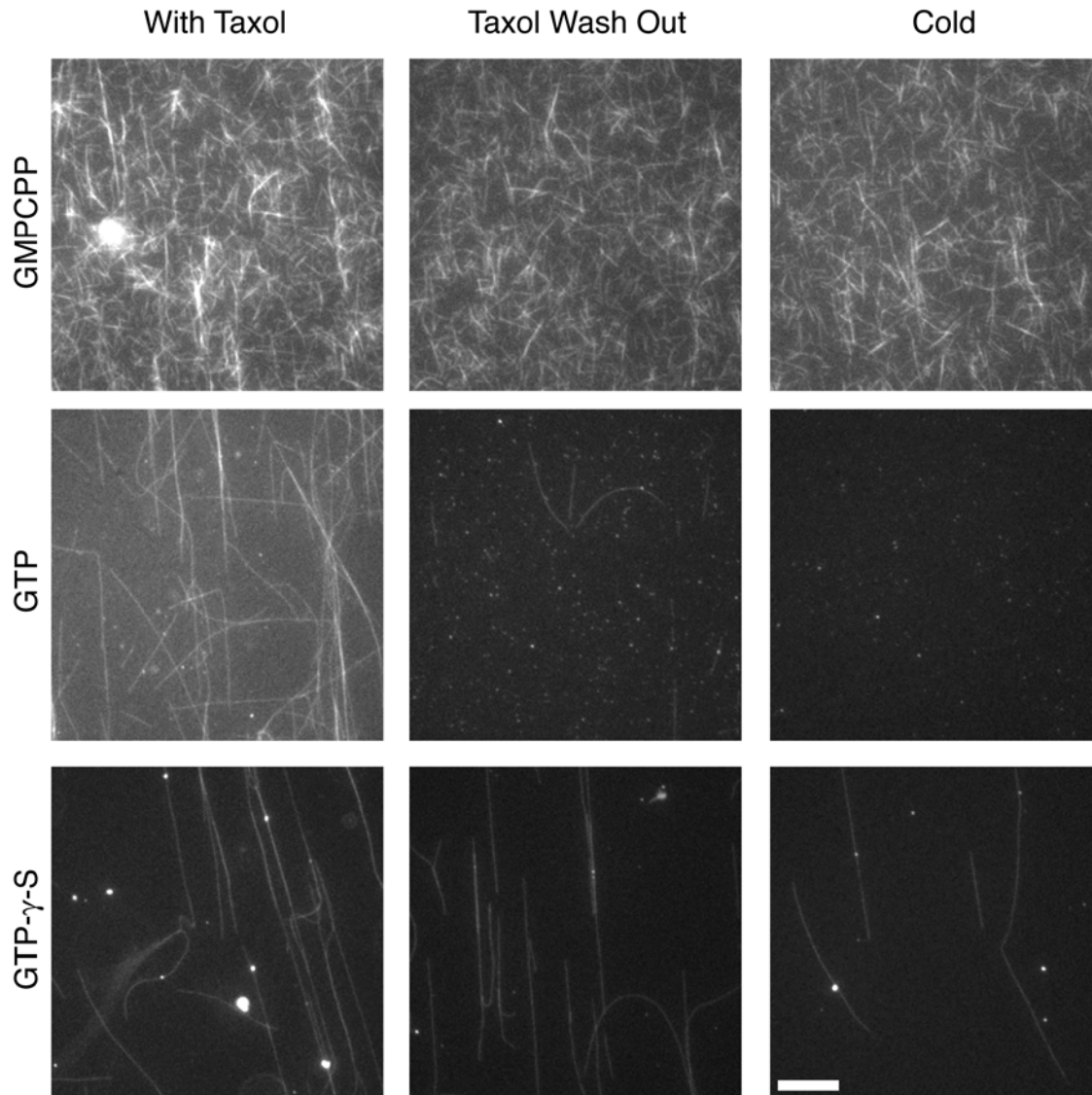
SUPPLEMENTAL FIGURES

Supplemental Figure 1
Hawkins et al



Supplemental Figure 1. Persistence length does not depend on the contour length of the filament. Persistence length as a function of filament contour length for data taken on microtubules (A) with Taxol only, (B) with GMPCPP, (C) with GMPCPP with Taxol, (E) GTP-g-S, (F) GTP-g-S with Taxol, (G) MAP4 with Taxol, (H) polymerized with tau, and (I) with tau added after Taxol. We have plotted each data set separately on different axes to show that none of our data has a length-dependent persistence length. We fit each data set to a linear function of the form: $y = mx + b$. (D) The fit parameter of the slope with the error of the fit for each data set.

Hawkins, et al. Supplemental Figure 2



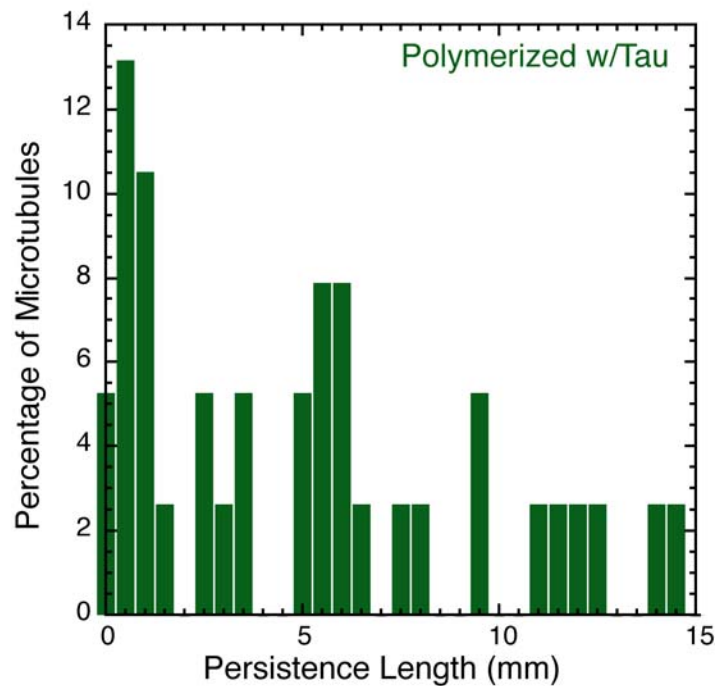
Supplemental Figure 2. GTP- γ -S microtubules are stable to dilution of Taxol and tubulin, but not cold stable. We compared the ability of GTP- γ -S to stabilize microtubules after depletion of tubulin and Taxol or after incubation at 4°C using a flow chamber. Rhodamine-labeled microtubules were polymerized with GMPCPP, GTP- γ -S, or GTP, and then stabilized with 5 μ M Taxol. They were attached to the cover slip of a flow chamber using rigor mutant kinesin (kinesin-560 T99N), washed with PEM-100 with 5 μ M Taxol to remove unbound filaments, and imaged with an EM-CCD camera (“With Taxol”). All chambers showed microtubules. As previously reported, the GMPCPP microtubules were shorter than the GTP or GTP- γ -S microtubules because GMPCPP nucleates microtubules quickly. Next, 15 chamber volumes of PEM-100 without Taxol was flowed into the chamber, and the filaments were imaged again (“Taxol Wash Out”). The GMPCPP microtubules were still bound at high concentration. The GTP microtubules were obviously shorter and fewer in the chamber.

The GTP- γ -S microtubules still appeared long with as many microtubules as prior to the washout.

Finally, the flow chambers were incubated at 4°C for 10 minutes and imaged again. The GMPCPP microtubules were bound with high concentration of filaments. The GTP microtubules were completely gone from the chamber. The GTP- γ -S microtubules were obviously shorter with fewer microtubules bound to the cover glass.

The scale bar represented 10 μ m, and is the same for all images.

Supplemental Figure 3
Hawkins et al



Supplemental Figure 3. Histogram of microtubule persistence lengths for microtubules polymerized in the presence of tau at 1:100 and subsequently stabilized with Taxol and tau at 1:1. The distribution is inconsistent with a normal, Gaussian distribution ($D = 0.68$, $p = 2.2 \times 10^{-16}$). It is also inconsistent with a log-normal distribution ($D = 0.51$, $p = 7.7 \times 10^{-10}$).

Supplemental Table 1. Parameters for Gaussian fits of Log-transformed histograms.

Data Set	Amplitude, A	Mean, x_0	Standard Deviation, σ	Goodness of fit, R^2
Taxol	43 ± 1	-0.50 ± 0.03	0.90 ± 0.03	0.99
GMPCPP	34 ± 5	0.3 ± 0.2	1.2 ± 0.2	0.85
GMPCPP+Taxol	37 ± 4	0.3 ± 0.1	1.0 ± 0.1	0.93
GTP- γ -S	48 ± 5	-1.02 ± 0.1	0.9 ± 0.1	0.94
GTP- γ -S+Taxol	48 ± 2	-0.82 ± 0.04	0.79 ± 0.04	0.99
Tau Added Before Polymerization	31 ± 3	1.5 ± 0.2	1.3 ± 0.2	0.93
Tau Added After Polymerization	46 ± 0.2	-0.76 ± 0.01	0.87 ± 0.01	1.00
MAP4+Taxol	78 ± 5	-0.43 ± 0.05	0.45 ± 0.05	0.98

Supplemental Table 2. Parameters for Gaussian fits of histogram for MAP4.

Data Set	Amplitude, A	Mean, x_0	Standard Deviation, σ	Goodness of fit, R^2
Taxol	10 ± 2	0.49 ± 0.29	0.66 ± 0.37	0.18
MAP4+Taxol	30 ± 4	0.59 ± 0.02	0.12 ± 0.02	0.79